

# Fat-constrained QSM for Abdominal Applications

Debra E. Hornig<sup>1,2</sup>, Diego Hernando<sup>1</sup>, Samir D. Sharma<sup>1</sup>, and Scott B. Reeder<sup>1,2</sup>

<sup>1</sup>Radiology, University of Wisconsin-Madison, Madison, WI, United States, <sup>2</sup>Medical Physics, University of Wisconsin-Madison, Madison, WI, United States

**Target audience:** Researchers interested in quantitative susceptibility mapping (QSM) for abdominal applications.

**Purpose:** Measurement of magnetic susceptibility has multiple applications in MRI, including iron quantification and assessment of cerebral microbleeds<sup>1</sup>. QSM techniques are based on estimating the susceptibility distribution from a measured  $B_0$  field map<sup>2</sup>. Unfortunately, the measured  $B_0$  field map is a superposition of both the background field, which is attributable to shim fields, and the susceptibility-induced field. The background field is often removed in brain applications by high pass filtering or estimation of spherical harmonics, but these techniques may not be applicable in the abdomen since iron can accumulate diffusely in large organs such as the liver and spleen, rather than in focal deposits. Further, the estimation of the susceptibility distribution involves an *ill-posed deconvolution process*, and generally has no unique solution. This challenge has been addressed in brain applications using techniques such as  $\ell_1$ -regularization<sup>3</sup>; however, these methods have not been validated in the abdomen. Unlike in the brain, the presence of fat (and air) in the abdomen also has the potential to constrain QSM estimation by assuming that their magnetic susceptibilities are known (constant) even in the presence of hepatic iron overload. The *purpose of this work* is to compare  $\ell_1$  regularization with a fat/air-constraint, to assess the accuracy of each method for body QSM in the presence of background field variation and noise.

**Methods:** A susceptibility distribution was created that contained regions mimicking air, subcutaneous fat, and two values of iron-overloaded tissue (Fig. 1a). The susceptibility distribution was used to create a susceptibility-induced  $B_0$  field map according to Koch et al.<sup>4</sup> A simulated background field was created as a 3<sup>rd</sup>-degree polynomial (Fig. 1b) of different levels (0,  $\pm 10$ Hz,  $\pm 20$ Hz, ...,  $\pm 100$ Hz) and was added to the susceptibility-induced field map to create a composite  $B_0$  field map. Fat and water signals were created to match the susceptibility boundaries. The fat and water signals, along with the composite field map, were used to create synthetic echo time images. Complex additive Gaussian noise of different power (SNR =  $\infty$ , 30, 15) was added to the synthetic echo time images. The noisy images were processed using a fat/water reconstruction algorithm<sup>5</sup> to obtain estimated fat, estimated water, and estimated  $B_0$  field map. These parameters were used as inputs to two different QSM algorithms:

1. A *fat- and air-constrained method*, which regularized the least-squares estimation by imposing known susceptibility values in regions of fat and air. Mathematically, the constraint is expressed as:

$$[B_0]_{\text{issue}} = [D\chi]_{\text{issue}}, \text{ subject to } [\chi]_{\text{fat}} = -7.79 \times 10^{-6}, [\chi]_{\text{air}} = 0.00$$

where  $[B_0]_{\text{issue}}$  denotes the measured  $B_0$  offset map over the “tissue” regions (i.e., excluding background air),  $D$  is the dipole response<sup>1</sup>, and  $[\chi]_{\text{fat}}$  and  $[\chi]_{\text{air}}$  denote the susceptibility distribution over fat and air regions, respectively.

2. An  $\ell_1$  regularization method<sup>3</sup>, which promoted piecewise constancy of  $\chi$ . See Fig. 2 for a flowchart of the process. An ROI was placed in the central region of the estimated susceptibility distributions, where the true susceptibility is  $-4.00$  ppm (Fig. 1a). The mean of the estimates within the ROI was compared between  $\ell_1$  regularization and fat/air-constrained fitting, across different background variation levels and different SNR levels (Fig. 3).

**Results:** At infinite SNR, both  $\ell_1$  regularization and fat/air-constrained fitting perform well across all background variation levels. However, for the realistic SNRs of 30 and 15, *fat/air-constrained fitting results in more accurate measurements* for all background variation levels.

**Discussion:** Fat/air-constrained fitting performs more accurately than  $\ell_1$  regularization in our simulations. The two methods may be combined in order to benefit from each simultaneously.

**Conclusion:** Exploiting information about the distribution of fat provides an opportunity to improve the accuracy of QSM in abdominal applications.

**References:** 1. Liu T et al. *Radiology*. 2012;262(1):269-278. 2. Haacke EM et al. *MRI*. 2005;23(1):1-25. 3. de Rochefort et al. *MRM*. 2008;60(4):1003-9. 4. Koch K et al. *Phys Med Biol*. 2006;51(24):6381-6402. 5. Hernando D et al. *MRM*. 2010;64(3):811-822.

**Acknowledgements:** We gratefully acknowledge support from the NIH (RC1 EB010384, R01 DK083380, R01 DK088925, and R01 DK096169) and the Wisconsin Alumni Research Foundation (WARF) Accelerator Program. We also wish to thank GE Healthcare for their support.

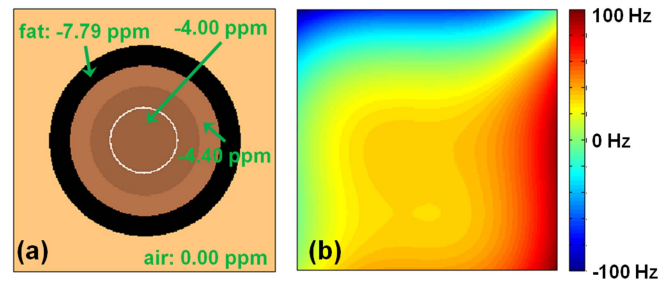


**Figure 1.** (a) Susceptibility distribution for the digital phantom. The white circle represents the ROI that was used to measure the mean of the estimated susceptibility. (b) Background field variation for  $\pm 100$  Hz, over the same area as the susceptibility distribution in (a).

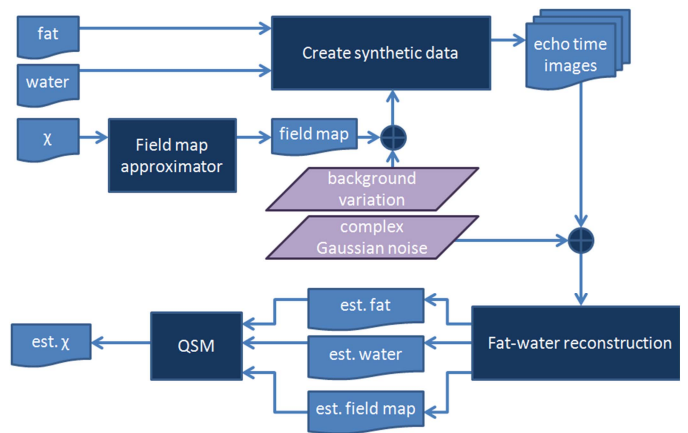


**Figure 2.** Flowchart for testing different QSM methods with synthetic data. The light blue boxes are data and the dark blue boxes represent filters or reconstructions. Background variation and complex Gaussian noise, represented by the purple boxes, simulate realistic conditions. The “QSM” box may be one of the two methods tested in this work:  $\ell_1$  regularization or fat/air constraints.

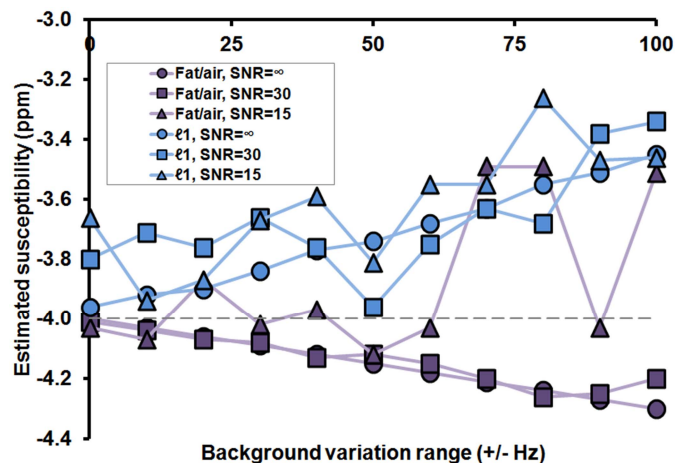


**Figure 3.** Fat/air-constrained fitting results in more accurate susceptibility measurements than  $\ell_1$  regularization. Fitting with  $\ell_1$  regularization results in measurements further away from the true susceptibility of  $-4.00$  ppm for both of the realistic SNR levels tested, and all background variation levels.